Biomech Model Mechanobiol (2009) 8:141–148
DOI 10.1007/s10237-008-0124-3

ORIGINAL PAPER

Determination of human arterial wall parameters from clinical data

Jonas Stålhand

Received: 7 December 2007 / Accepted: 27 February 2008 / Published online: 18 March 2008

Abstract This study suggests a method to compute the material parameters for arteries in vivo from clinically registered pressure-radius signals. The artery is modelled as a hyperelastic, incompressible, thin-walled cylinder and the membrane stresses are computed using a strain energy. The material parameters are determined in a minimisation process by tuning the membrane stress to the stress obtained by enforcing global equilibrium. In addition to the mechanical model, the study also suggests a preconditioning of the pressure-radius signal. The preconditioning computes an average pressure-radius cycle from all consecutive cycles in the registration and removes, or reduces, undesirable disturbances. The effect is a robust parameter identification that gives a unique solution. The proposed method is tested on clinical data from three human abdominal aortas and the results show that the material parameters from the proposed method do not differ significantly ($p < 0.01$) from the corresponding parameters obtained by averaging the result from consecutive cycles.

Keywords Abdominal aorta · Continuum model · In vivo · Mechanics · Parameter identification

1 Introduction

One of the major objectives of cardiovascular research is to learn more about the interaction of the different constituents that comprises the system. In this knowledge resides the key to understanding important processes such as ageing and development of diseases, both closely related to the mechanics of the soft tissue. For instance, it is generally accepted that the abdominal aorta stiffens with age (Länne et al. 1992; Sonesson et al. 1993). This is believed to be related to fibrosis and progressive depositions of amorphous substances for the elastin (Nichols and O'Rourke 2005) and to increased cross-linking for collagen (Bailey et al. 1998). These processes reduce the mobility of the constituents, for instance, the increased cross-linking of collagen with age restrains the unfolding of the molecule and the arterial wall stiffens.

Several studies have tried to assess the mechanical properties of the normal and the diseased arterial wall. The most detailed are in vitro studies in which both the global response and the micro structural changes to different loads and stimuli can be assessed, see, for instance, Cattell and Anderson (1996), Holzapfel et al. (2005), and Schulze-Bauer et al. (2003). These studies are of great importance since they provide information which can be used to develop new models. However, a weakness of all in vitro studies is that the specimen is deprived of its environment, e.g. the periadventitial support and different chemical and hormonal stimuli. In addition, in vitro studies are also impossible to use clinically since they require dissection of the specimen. Other studies have tried to assess the mechanical properties in vivo, see for instance, Ryden-Ahlgren et al. (2001), Hansen et al. (1995), Länne et al. (1992), and Sonesson et al. (1993). Therein, the arterial wall stiffness is estimated by the pressure strain elastic modulus (Peterson et al. 1960) or the, so-called, stiffness (Kawasaki et al. 1987). Although appealingly simple, the measures suffer from a weakness: they are based on the global pressure-radius response of the arteries while the cause is related to the micro structure. The need for a more detailed in vivo method that links the global response to the underlying structure is, therefore, evident.

J. Stålhand (✉)
Division of Mechanics, Linköping Institute of Technology,
581 83 Linköping, Sweden
e-mail: jonas.stalhand@liu.se

Attempts at developing a detailed method for the in vivo situation has been presented before, see Schulze-Bauer and Holzapfel (2003) and previous work from our research group (Stålhand and Klarbring 2005, 2006; Stålhand et al. 2004). Methods for the in vivo case must handle a couple of complications that are not present for the in vitro case. First, the data to the model are often incomplete in the sense that only the pressure-radius response is registered excluding all information in the axial direction of the vessel. In addition, the registration time is often limited for practical reasons and, therefore, the number of available pulses. Second, data collected under in vivo conditions are often afflicted by disturbances, e.g., respiratory motion and involuntary movements of the ultrasonic probe. An example can be seen in the last radii cycles in Fig. 1 where the hand-held ultrasonic probe is slightly shifted and loses focus; a measurement error is, thereby, introduced. The effect of the measurement error is a deterioration of the parameter identification process, resulting in large variations of the parameters identified from consecutive pulses, as will be shown. An intuitive solution is to use the mean of the parameters. The mean may not be a good choice in all situations, however, since it is sensitive to outliers. This problem is further aggravated by the limited number of pulses. This study addresses the identification issues outlined above and proposes a method to obtain a unique set of material parameters. The method comprises a signal processing routine and a mechanical model. The signal processing routine removes noise, corrects any offset between the pressure and radius signals, and computes an average, or system, shape for the registered pulses. The result is then fed to a mechanical model which approximates the artery as a thin-walled, homogeneous cylinder and computes the membrane stresses using a two-dimensional form of the strain-energy function proposed by Holzapfel et al. (2000). The membrane stresses are determined down to a set of unknown material and geometrical parameters. These parameters are obtained by a least-squares fitting of the membrane stresses and the stresses computed by enforcing global equilibrium. Since the parameter identification operates on the average shape, a unique set of model parameters are obtained for each subject and the problems associated with the mean are not encountered.

2 Method

The mechanical model and the signal processing routine are described in the following subsections. Two sets of stresses are determined for the mechanical model: equilibrium stresses and constitutively determined stresses. These sets are then used in the parameter identification where the underlying idea is that the membrane stress computed in the two different ways should be equal.

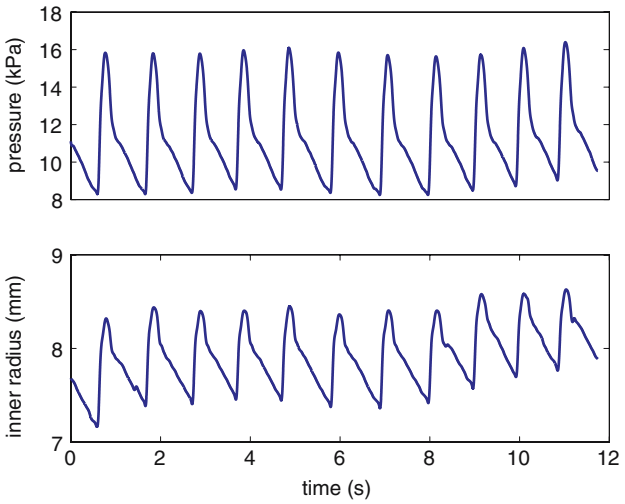

Fig. 1 A typical clinical registration of the pressure and radius. Note the measurement error in the radius signal at the end of the registration (the strong coning of the cycles in the interval 8–12 s)

2.1 Equilibrium stress

Let the abdominal aorta be given by a thin-walled, incompressible cylinder of length l, and inner and outer radius r_0 and r_1, respectively. The cylinder is subjected to a pressure at the inner boundary while the outer boundary is traction free.

By enforcing global equilibrium, the circumferential and axial stress are computed to be:

$$\sigma_{\theta\theta} = \frac{P(r_1 + r_0)}{2h}, \quad \sigma_{zz} = \frac{\pi r_0^2 P + F}{A}, \tag{1}$$

where P is the transmural pressure, $h \ll r_0$ is the wall thickness, F is the external axial force (equal to the force measured in in vitro inflation tests) and A is the current wall cross-sectional area. The outer radius and wall thickness can be eliminated from the circumferential stress using the relations $A = 2\pi r_0 h$ and $r_1 = r_0 + h$. After the elimination the membrane stresses become

$$\sigma_{\theta\theta} = \left(\frac{2\pi r_0^2}{A} + \frac{1}{2}\right) P, \quad \sigma_{zz} = \frac{\pi r_0^2 P + F}{A}. \tag{2}$$

To compute the membrane stresses, two assumptions need to be made (Schulze-Bauer and Holzapfel 2003),

(i) the axial force and the axial stretch are constant and independent of the internal pressure, and
(i) the ratio between the axial and circumferential stress is known at one internal pressure $\overline{P}$.

The axial force in Eq. (2)^2 can be determined explicitly by applying condition (ii). If the ratio $\gamma = \sigma_{zz}/\sigma_{\theta\theta}$ is known at the pressure $\overline{P}$, the axial force is given by:

$$F = \pi \bar{r}_0^2 \overline{P} \left(2\gamma + \frac{\gamma A}{2\pi \bar{r}_0^2} - 1 \right), \tag{3}$$

where $\bar{r}_0$ is the inner radius corresponding to $\overline{P}$. Note that Eqs. (2) and (3) do not depend on the material properties of the vessel. They are only functions of the applied load and geometry, and, as a consequence, the membrane stress becomes statically determined.

2.2 Constitutively determined stress

In addition to the loaded state previously described, introduce an unloaded, stress-free reference state. Let the reference state be a thin-walled cylinder of length L, and inner and outer radius R_0 and R_1, respectively. The deformation out of the reference state is described by the deformation gradient

$$\mathsf{F} = \lambda_\theta \mathbf{E}_\theta \otimes \mathbf{E}_\theta + \lambda_z \mathbf{E}_z \otimes \mathbf{E}_z + \lambda_r \mathbf{E}_r \otimes \mathbf{E}_r, \tag{4}$$

where λ_θ, λ_z, and λ_r are the stretches, and $\mathbf{E}_\theta$, $\mathbf{E}_z$, and $\mathbf{E}_r$ are the cylindrical base vectors. The indices θ, z, and r denote the circumferential, axial, and radial directions, respectively. For future use we also introduce the right Cauchy-Green stretch tensor defined as $\mathsf{C} = \mathsf{F}^{\mathrm{T}}\mathsf{F}$ where a superscribed T denotes the transpose. The stretches in Eq. (4) are not independent since the arterial wall is incompressible. The stretches must, therefore, satisfy the incompressibility constraint

$$\det \mathsf{F} = \lambda_\theta \lambda_z \lambda_r = 1. \tag{5}$$

The stress tensor for an hyperelastic, incompressible material is given by (Holzapfel 2000)

$$\sigma^{\mathrm{mod}} = -p\mathsf{I} + \mathsf{F}\frac{\partial \psi}{\partial \mathsf{C}}\mathsf{F}^{\mathrm{T}}, \tag{6}$$

where p is an arbitrary multiplier associated with the incompressibility, I is the identity tensor, and ψ is the strain energy. The superscript mod indicates that the stresses are associated with the continuum model. Following Holzapfel et al. (2000), we take the strain energy function to be additively decomposed into an isotropic part ψ_{iso} associated with the non-collageneous materials such as elastin, smooth muscle cells, and other cellular and non-cellular material, and an anisotropic part ψ_{ani} associated with the embedded collagen fibres. Thus,

$$\psi = \psi_{\mathrm{iso}} + \psi_{\mathrm{ani}}. \tag{7}$$

In addition, let the collagen fibres be oriented along the two (non-parallel) direction vectors $\mathbf{M}$ and $\mathbf{N}$ in the reference state and introduce the particular strain-energy functions suggested in Holzapfel et al. (2000):

$$\begin{aligned} \psi_{\mathrm{iso}} &= c(I_1 - 3), \\ \psi_{\mathrm{ani}} &= \frac{k_1}{2k_2}\left(e^{k_2(I_4-1)^2} + e^{k_2(I_6-1)^2} - 2 \right), \end{aligned} \tag{8}$$

where $I_1 = \mathrm{tr}\,\mathsf{C}$, $I_4 = \mathbf{M}\cdot\mathsf{C}\mathbf{M}$, $I_6 = \mathbf{N}\cdot\mathsf{C}\mathbf{N}$. The constants must satisfy $c, k_1, k_2 > 0$ to guarantee material convexity. Let the collagen fibres be oriented in two concentric helices, symmetrically arranged around the circumferential direction. If the pitch angle relative to the circumferential direction is β, the fibre direction vectors are given by:

$$\mathbf{M} = \cos\beta\,\mathbf{E}_\theta + \sin\beta\,\mathbf{E}_z, \quad \mathbf{N} = \cos\beta\,\mathbf{E}_\theta - \sin\beta\,\mathbf{E}_z. \tag{9}$$

The average radial stress in a thin-walled cylinder can be approximated by $-Pr_0/(r_0 + r_1)$ (Humphrey 2002) and is at least one order-of-magnitude smaller than the other membrane stresses, c.f., Eq. (1). The radial stress is, therefore, taken to be $\sigma_{rr} = \sigma_{rr}^{\mathrm{mod}} \approx 0$. The arbitrary multiplier p can now be determined by substituting Eqs. (4) and (7)–(9) in Eq. (6) and applying $\sigma_{rr}^{\mathrm{mod}} = 0$. The result reads $p = 2c\lambda_r^2 = 2c(\lambda_\theta\lambda_z)^{-2}$, where the last equality follows from Eq. (5). Back-substitution of the result into Eq. (6) gives the circumferential and axial stress

$$\begin{aligned} \sigma_{\theta\theta}^{\mathrm{mod}} &= 2c\left(\lambda_\theta^2 - \frac{1}{(\lambda_\theta\lambda_z)^2}\right) + 4k_1(I-1)e^{k_2(I-1)^2}\lambda_\theta^2(\cos\beta)^2, \\ \sigma_{zz}^{\mathrm{mod}} &= 2c\left(\lambda_z^2 - \frac{1}{(\lambda_z\lambda_\theta)^2}\right) + 4k_1(I-1)e^{k_2(I-1)^2}\lambda_z^2(\sin\beta)^2, \end{aligned} \tag{10}$$

where $I = I_4 = I_6 = \lambda_\theta^2(\cos\beta)^2 + \lambda_z^2(\sin\beta)^2$.

In order to compute the model stresses for a given set of material parameters, c, k_1, k_2, and β, we must define the stretches λ_θ and λ_z. Let the stretches in the mid-wall be defined as

$$\lambda_\theta = \frac{r_1 + r_0}{R_1 + R_0}, \quad \lambda_z = \frac{l}{L}.$$

The outer radii can be eliminated from the circumferential stretch in analogy with the method used for Eq. (2). Take the referential cross-sectional wall area to be $A_0 = 2\pi R_0 H$, where H is the referential wall thickness, and use $R_1 = R_0 + H$ to arrive at

$$\lambda_\theta = \frac{R_0}{r_0}\frac{4\pi r_0^2 + A}{4\pi R_0^2 + A_0}.$$

The referential and current cross-section areas are related through the incompressibility constraint. Incompressibility implies constant volume for the vessel wall and, hence, $Al = A_0 L$. By substituting Al/L for A_0 and using that $\lambda_z = l/L$, the stretches can be written as

$$\lambda_\theta = \frac{R_0}{r_0}\frac{4\pi r_0^2 + A}{4\pi R_0^2 + \lambda_z A}, \quad \lambda_z = \frac{l}{L}. \tag{11}$$

For a given set of material parameters, the membrane $\sigma_{\theta\theta}^{\text{mod}}$ and σ_{zz}^{mod} can now be computed by substituting Eq. (11) in Eq. (10).

2.3 Signal processing routine

To improve the performance of the method, the measured signals are subjected to a preconditioning step prior to the identification process. The preconditioning step has the objective to remove, or reduce, disturbances in the signals that deteriorates the parameter identification. The disturbances are typically noise, respiratory artifacts, and errors introduced by small, involuntary movements of the ultrasonic probe. Albeit not related to the mechanical model itself, this step is crucial in order to have robust parameter identification, see Sect. 5. The preconditioning step suggested in this subsection is suitable for implementation as an automatic routine prior to the parameter identification.

The measurement consists of simultaneous registrations of the internal pressure and the inner radius at a uniform sampling time T. First, the signals are zero-phase filtered through a low-pass fourth-order Butterworth filter to remove noise. The cut-off frequency of the filter is chosen to be 15 Hz following Fetics et al. (1999).

Second, the pressure and radius signals are re-aligned in the time domain to remove an offset associated with the measurement setup, see Sonesson et al. (1994). The offset is automatically estimated using a low-order ARX model (autoregressive exogenous model, see Ljung 1999). The ARX model is based on a linear difference equation relating the output $y(t)$ and the input $u(t)$ according to

$$\begin{aligned} y(t) + a_1 y(t-T) + \cdots + a_{n_a} y(t-n_a T) \\ = b_1 u(t-(n_k+1)T) + \cdots + \\ b_{n_b} u(t-(n_k+n_b)T) + e(t), \end{aligned} \tag{12}$$

where the output $y(t)$ depends on the n_a previous outputs, the n_b previous inputs delayed n_k samples, and the error term $e(t)$. The parameters a_k $(k = 1, \ldots, n_a)$ and b_l $(l = 1, \ldots, n_b)$ in Eq. (12) can be computed using linear regression for a given model order and delay (Ljung 1999). An estimate of the offset is obtained in the following way: the pressure and radius signals are chosen as output and input to the ARX model, respectively. After a suitable scaling where the signals are given the same order of magnitude, the linear regression is computed for different delays using an ARX model of order $n_a = 1$ and $n_b = 2$. The offset is taken to be the delay with the lowest residual. The particular ARX model chosen in this case corresponds to a classical viscoelastic three-parameter element, c.f., Flügge (1975). This element is able to separate the offset associated with the measurement setup from the time delay associated with the intrinsic viscoelastic properties of the wall. In this way, the correction does not affect the offset associated with the viscoelasticity.

Third, the pressure and radius signals are segmented into consecutive pulses after the re-alignment. The segmentation is done by computing the second derivative of the pressure signal with respect to time using a central difference formula. At the onset of the systolic (loading) flank, the second derivative has a characteristic peak-up–peak-down pattern that is used as a trigger. The minimum pressure is sought in a window around the trigger and stored. A complete pulse cycle is then defined as the samples between two pressure minima.

Fourth, average pulses for the pressure and the radius signals are computed for each subject using the segmented pulses. The average pulse is computed using a method called corrected integral shape averaging (CISA), see Boudaoud et al. (2007).

Finally, the average pressure-radius loop is re-sampled from time equidistant to path equidistant samples along the averaged pressure-radius loop using cubic interpolation. Path equidistant samples give the same weight to the whole pressure-radius cycle in the parameter identification and avoids the higher weight implicitly placed on parts with slower dynamics by time equidistant sampling, see Stålhand et al. (2004).

2.4 Parameter identification

Let the processed radius and pressure signals, r_0 and P, respectively, be the input to the mechanical model defined by Eqs. (10) and (11). The mechanical model is determined down to the model parameters R_0, λ_z, c, k_1, k_2, β, and the cross-sectional area A. These parameters must be obtained by a parameter identification process. The cross-sectional area was not available for the data at hand but it is, in principle, measurable using ultrasonic equipment. It will, therefore, be eliminated using published data for the intima-media-complex in humans, see Sect. 3.

The parameters can be computed by applying standard minimisation techniques. For instance, define the objective function as the sum of squared errors for the membrane stresses as

$$\begin{aligned} \phi(\boldsymbol{\kappa}) = \sum_{j=1}^{n} \Big[\Big(\sigma_{\theta\theta}^{\text{mod}}(\boldsymbol{\kappa}, r_{0,j}) - \sigma_{\theta\theta}(r_{0,j}, P_j) \Big)^2 + \\ \Big(\sigma_{zz}^{\text{mod}}(\boldsymbol{\kappa}, r_{0,j}) - \sigma_{zz}(r_{0,j}, P_j) \Big)^2 \Big], \end{aligned} \tag{13}$$

where $\boldsymbol{\kappa} = (R_0, \lambda_z, c, k_1, k_2, \beta)$ is a vector, j denotes a sample, and n is the total number of samples in the average pulse. The model parameters are then the solution to the minimisation problem:

$$\begin{cases} \min\limits_{\boldsymbol{\kappa}} \phi(\boldsymbol{\kappa}) \\ \text{subject to: } \underline{\boldsymbol{\kappa}} \leq \boldsymbol{\kappa} \leq \overline{\boldsymbol{\kappa}}, \end{cases}$$

where $\underline{\boldsymbol{\kappa}}$ and $\overline{\boldsymbol{\kappa}}$ are the lower and upper bounds for $\boldsymbol{\kappa}$, respectively. The standard function *fmincon* in the Matlab Optimization Toolbox (The Mathworks, Natick, MA, USA) is used to solve the minimisation problem in this study. The exact jacobian for the objective function $\phi(\boldsymbol{\kappa})$ is supplied to enhance the robustness and convergence rate of the parameter identification process.

3 Material

The material for this study is three healthy, non-smoking, Caucasian males, see Table 1. The pressure was measured invasively using a catheter while the radius was obtained non-invasively through an echo-tracking system. For a detailed description of the material and the measurements, see Sonesson et al. (1994). Informed consent was given by each subject prior to investigation.

The current wall cross-sectional area was not available for the data at hand. It was instead approximated by the intima-media area in the male human abdominal aorta obtained from Åstrand et al. (2005). To account for the adventitial thickness, it was assumed that the intima-media-complex comprises two-third of the wall thickness (Holzapfel et al. 2000). After correction, the current wall cross-sectional area is given by: $A = 19.60 + 0.80 \times \text{age}(p < 0.0001)$, where A is in mm^2 and age is in years.

4 Results

The method described in Sect. 2 is applied to the subjects in Table 1. The stress ratio is taken to be $\gamma = 0.59$ at the pressure $\overline{P} = 13.3\,\text{kPa}$ following Schulze-Bauer and Holzapfel (2003). There is no unique pressure-radius relation because of the hysteresis, and the associated inner radius $\overline{r}_0$ is taken to be the average of the two flanks at $\overline{P}$. The lower bounds for R_0, c, k_1, and k_2 are set to 10^{-8} to guarantee strictly positive values. The lower and upper bounds on λ_z are set to 1.0 and 1.3, respectively, the former chosen to avoid buckling and the latter as a physiological upper limit, see Stålhand et al. (2004). Note, however, that axial stretch under 1.0 has been observed in elderly (Schulze-Bauer et al. 2003). The bounds for the fibre angle is taken to be $10^{-8} \leq \beta \leq \pi/2$ to guarantee non-parallel fibre vectors.

Table 1 Data for the subjects used in the method

Subject	Age (years)	Length (cm)	Weight (kg)	DBP (kPa)	SBP (kPa)
I	41	MI	MI	9.6	16.1
II	25	191	83	8.4	15.8
III	24	168	67	9.4	16.8

DBP and SPB are the diastolic and systolic blood pressures, respectively, MI missing information

Table 2 Model parameters computed by using the average cycle from the CISA method

Subject	R_0 (mm)	λ_z (–)	c (kPa)	k_1 (kPa)	k_2 (–)	β (deg)
I	5.61	1.08	34.40	10.31	5.61	46.1
II	5.86	1.05	18.80	44.20	2.56	45.7
III	5.53	1.04	40.86	20.92	4.41	50.2

Table 3 Model parameters computed by taking the average of the parameters obtained for the consecutive cycles (mean ± 1SD)

Subject	No. cycles	R_0 (mm)	λ_z (–)	
I	10	5.65 ± 1.36	1.12 ± 0.07	
II	10	4.74 ± 1.65	1.09 ± 0.11	
III	9	5.46 ± 0.20	1.05 ± 0.01	
Subject	c (kPa)	k_1 (kPa)	k_2 (–)	β (deg)
I	26.49 ± 14.07	7.32 ± 4.20	4.73 ± 3.73	47.2 ± 2.2
II	21.74 ± 28.26	21.26 ± 16.48***	3.60 ± 14.26	49.7 ± 5.48
III	38.70 ± 8.49	21.16 ± 4.94	4.31 ± 1.57	50.2 ± 0.65

*** significant difference compared to the parameter in Table 2 at the $p < 0.001$ level

The model parameters are computed in two different ways: first, using the average cycle from the CISA method described in Sect. 2.3, and, second, by identifying a set of model parameters for each consecutive cycle and taking the mean of all cycles. The results are presented in Tables 2 and 3.

The parameters in Table 3 are tested to see if there is any significant difference compared to the parameters in Table 2 using a paired t-test. Values of $p < 0.01$ are considered significant. The results show that there is no significant difference in the parameters identified using the CISA cycle or the mean parameters from the consecutive cycles, apart from k_1 for subject II. The p-value and the confidence intervals from the t-test are presented in Table 4 for completeness.

Finally, the membrane stresses are computed using the values in Table 2 and the result is presented in Figs. 2, 3 and 4. The physiological condition for each subject is indicated by a bar.

5 Discussion

A comparison of the parameters obtained using the average cycle in Table 2 and the mean of the parameters from the consecutive cycles in Table 3 shows reasonable agreement,

Table 4 The p-value and the 99% confidence interval (CI) from a paired t-test to compare the parameters computed by the CISA method to the those computed by taking the average of the consecutive cycles

Subject	R_0 (mm)	λ_z (–)		
I	p 0.115	0.078		
	CI [−0.51, 1.88]	[−0.10, 0.02]		
II	p 0.094	0.254		
	CI [−0.58, 2.42]	[−0.15, 0.06]		
III	p 0.307	0.723		
	CI [−0.12, 0.26]	[−0.01, 0.01]		
Subject	c (kPa)	k_1 (kPa)	k_2 (–)	β (deg)
I	p 0.114	0.337	0.440	0.151
	CI [−5.19, 19.40]	[−3.34, 6.84]	[−2.32, 4.08]	[−2.92, 0.92]
II	p 0.316	0.0001	0.250	0.047
	CI [−34.94, 16.52]	[9.94, 39.94]	[−18.34, 7.62]	[-8.69, 1.29]
III	p 0.458	0.888	0.853	0.464
	CI [−6.11, 10.42]	[−5.04, 4.57]	[−1.43, 1.63]	[−0.79, 0.47]

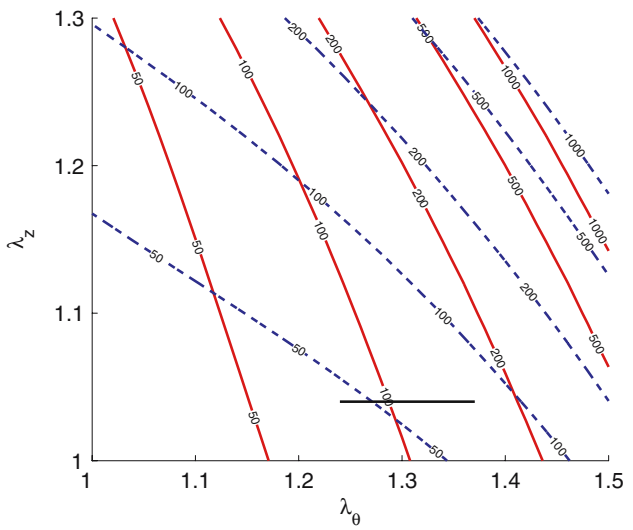

Fig. 2 The membrane stress in the abdominal aorta wall as a function of the stretches for subject I. *Solid* and *dashed lines* are the tangential and axial stress, respectively, at, from left to right, 50, 100, 200, 500, and 1000 kPa. The *vertical bar* indicates the physiological range for the subject

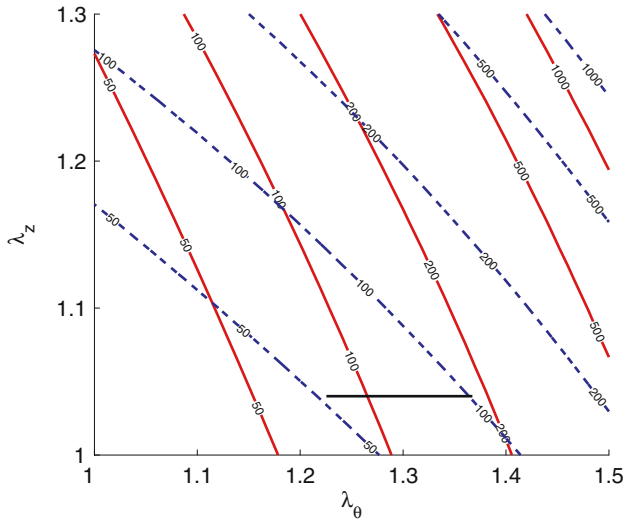

Fig. 3 The membrane stress in the abdominal aorta wall as a function of the stretches for subject II. Plot key same as in Fig. 2

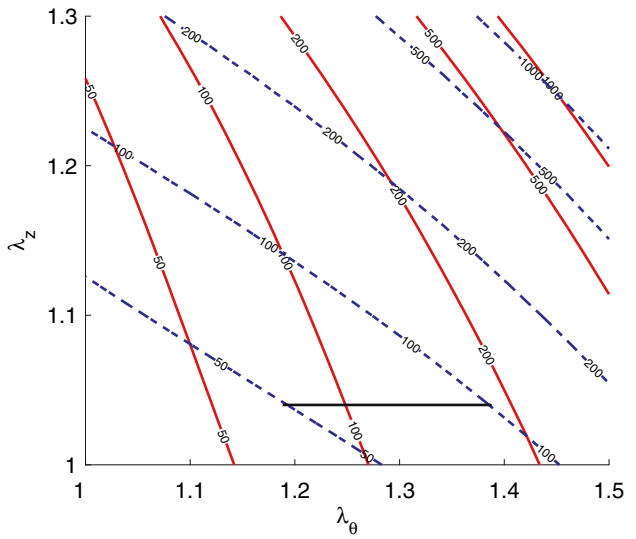

Fig. 4 The membrane stress in the abdominal aorta wall as a function of the stretches for subject III. Plot key same as in Fig. 2

an observation also corroborated by the t-test. This is in particular true for subject III who has notably uniform pressure-radius cycles, indicated by a small standard deviation for the parameters, in comparison with the others. For this subject, the mean of the parameters from the consecutive cycles is very close to the value from the average cycle. This result shows that the parameters obtained from the two methods converge as the intra cycle difference tends to zero, as expected. For subject II, on the other hand, the intra cycle variance is substantial, see Fig. 5. The variance causes a considerable difference for the material parameters in Table 3, as indicated by the large standard deviation, which can be expected since the parameter identification uses the pressure-radius response curve. On closer inspection, it can be seen that the pulses at both ends of the registration are affected by the measurement, see Fig. 1. If these pulses are removed and the average is recomputed by using cycles 2–7, the result becomes: $R_0 = 5.036 \pm 1.603$ mm, $\lambda_z = 1.030 \pm 0.023$, $C = 21.72 \pm 19.59$ kPa, $k_1 = 29.89 \pm 12.11$ kPa, $k_2 = 2.87 \pm 1.87$, and $\beta = 50.4 \pm 7.0$ (mean $\pm$ SD). The mean is closer to the values obtained using the average cycle but the standard deviations are of the same order as before, c.f., Table 3. This indicates that there still is a substantial variation among the parameters. However, there is no longer a significant

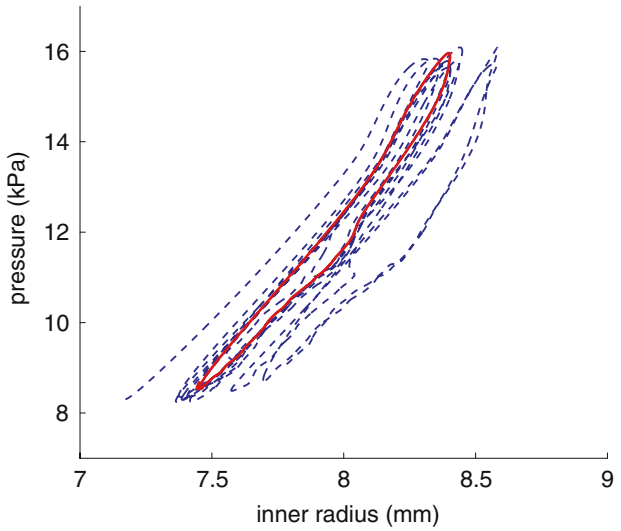

Fig. 5 Distribution of the consecutive pressure-radius cycles for subject II (*dashed lines*) and the average cycle (*solid line*)

difference between the mean values and the parameters from the average cycle in Table 2 when using a paired t-test.

The average cycle has two features which makes it attractive. First, it is a simple way to reduce the superimposed motion from respiration by averaging the effect from inhalation and exhalation. Second, the average cycle may be thought of as the underlying system cycle that the artery will have free of disturbances. This means that the parameters identified using the average cycle are a better representation of the true arterial properties than the average parameters from the consecutive cycles. This is because the parameters in the latter case also model possible measurement errors and respiratory artifacts. Finally, the cost for computing an average cycle, in terms of CPU time, is much smaller than the cost to compute the model parameters. The proposed method is, therefore, much cheaper.

The abdominal aorta is modelled as a cylindrical, homogeneous membrane in this study. In reality, this assumption is questionable. First, the wall thickness to radius ratio for arteries is, generally, greater than 0.1 (Nichols and O'Rourke 2005) and the aorta should be treated as thick wall cylinder. A thick walled theory is much more complex in terms of modelling and parameter identification, however (Stålhand et al. 2004), and this study is, therefore, confined to treating the aorta as a cylindrical membrane. Second, most arteries consist of three separate layers: tunica intima, tunica media, and tunica adventitia. Each layer has a unique constitution and mechanical properties (Holzapfel et al. 2000, 2005; Schulze-Bauer et al. 2002), and a truly correct model should treat them as separate layers and not assume the wall to be homogeneous. Although desirable, it does not seem feasible to introduce three layers in the in vivo case. The reason is that the clinically measurable pressure-radius response contains a limited amount of information from which the model parameters are identified. A threefold increase of the material parameters is likely to introduce dependencies among the model parameters resulting in an over-parameterisation of the objective function in Eq. (13). For a thorough discussion on the implication of over-parameterisation, see Stålhand et al. (2004).

In addition to the membrane assumption, the abdominal aorta is also assumed stress free in its unloaded case, implying that there is no residual stress in the tangential direction. The existence of a residual stress in arteries has been known for many years, and its major effect is to redistribute the stress field to achieve transmuraly uniform conditions at some pressure. For a membrane model, the effect of residual stress is only reflected by an increase in the stress level since the transmural distribution is not modelled in the two-dimensional analysis. The membrane stress may, therefore, be thought of as an average stress in the arterial wall and, in a first approximation, it is assumed equal to the uniform stress field caused by the residual stress. Furthermore, the outer boundary is taken to be traction free, i.e., the artery is a free-standing tube and the periadventitial support is neglected. If the surrounding tissue is assumed axisymmetric and its material properties are known, the periadventitial support can be modelled as an external pressure on the outer boundary of the artery. Singh and Devi (1990) used this approach to compute the stress difference in the circumferential direction between a tethered and a free artery. Their result indicates that the difference is small, about 10% or less of the total circumferential stress. Given the limited influence on the solution and that a correct model would also require an identification of the surrounding tissue's mechanical properties, the traction-free boundary was considered sufficient for this study, as a first approximation.

Although the mechanical modelling in this study is the same as in Schulze-Bauer and Holzapfel (2003), the strain energy functions differ. The reason to change from the Fung-type, exponential strain energy to the decoupled strain energy proposed in Holzapfel et al. (2000) is that the latter is more detailed in its description of the underlying structure by separating the isotropic and anisotropic constituents. In addition, the isotropic part of the strain energy in Eq. (8) proved important to get a good fit for the objective function in Eq. (13) for the young subjects, particularly at low pressures.

In a number of previous studies by the research group (Stålhand and Klarbring 2005, 2006; Stålhand et al. 2004), it has been observed that the parameter identification depends on the initial guess for κ. The parameter identification in this study was tested for this dependency by altering the initial guess for κ. Regardless of the initial guess, the identification process converged rapidly to the same solution (for the considered subject). This is taken as an indication of the existence of a unique local minimum within the bounds for κ

(mathematically this is equivalent to the objective function being unimodal). It is, therefore, possible to identify a unique set of model parameters and, as a consequence, a unique stress field in the arterial wall.

The anisotropy is introduced by the embedded fibres' orientation, i.e., the angle β. Because of the two-dimensional modelling, β becomes a phenomenological parameter and cannot be directly compared to histological data. The collagen fibre orientation is usually considered almost circumferential in the media while being more axial in the adventitia, see Holzapfel et al. (2000) and Rhodin (1980). If β in Table 2 is interpreted as the angle which gives the mean anisotropy of the two layers, values in the interval 45°–50° seem to be reasonable.

To assess the precision in the re-alignment of the pressure and radius signals by the ARX model, the offset for the subjects I–III were compared to a manual correction made by an experienced vascular chief surgeon. The comparison showed complete agreement for subjects II and III and a difference of six samples (0.007 s) for subject I. The ARX model was, therefore, considered acceptable for this purpose of this study. Other model orders for the ARX model were also tested, but the results were not as good.

In conclusion, this study presents a method suitable for in vivo estimation of material parameters from clinical measurements. The method reduces the effect of disturbances in the data by computing the model parameters from an average pressure-radius response. The study also shows that this average response is preferable in the parameter identification process.

Acknowledgements The author wishes to thank Håkan Åstrand, MD, and Toste Länne, MD, PhD, at the Department of Medical and Health Sciences at Linköping University for invaluable help and for providing data.

References

Åstrand H, Ryden-Ahlgren Å, Sandgren T, Länne T (2005) Age-related increase in wall stress of the human abdominal aorta: an in vivo study. J Vasc Surg 42:926–931

Bailey AJ, Paul RG, Knott L (1998) Mechanism of maturation and ageing of collagen. Mech Ageing Dev 106:1–56

Boudaoud S, Rix H, Meste O, Heneghan C, O'Brian C (2007) Corrected integral shape averaging applied to obstructive sleep apnea detection from the electrocardiogram. EURASIP J Adv Signal Process 2007:1–12, doi:10.1155/2007/32570

Cattell MA, Anderson JC (1996) Age-related changes in amounts and concentration of collagen and elastin in normotensive human thoracic aorta. Clin Chim Acta 245:73–84

Fectics B, Nevo E, Chen CH, Kass DA (1999) Parametric Model Derivation of Transfer Function for Noninvasive Estimation of Aortic Pressure by Radial Tonometry. IEEE Trans Biomed Engrg 46:698–706

Flügge W (1975) Viscoelasticity. Springer, New York

Hansen F, Mangell P, Sonesson B, Länne T (1995) Diameter and compliance in the human common carotid artery — variation with age and sex. Ultrasound Med Biol 21:1–9

Holzapfel GA (2000) Nonlinear solid mechanics, a continuum approach for engineering. Wiley, Chichester

Holzapfel GA, Gasser TC, Ogden RW (2000) A new constitutive framework for arterial wall mechanics and a comparative study of material models. J Elasticity 61:1–48

Holzapfel GA, Sommer G, Gasser TC, Regitnig P (2005) Determination of layer-specific mechanical properties of human coronary arteries with nonatherosclerotic intimal thickening and related constitutive modeling. Am J Physiol 289:H2048–H2058

Humphrey JD (2002) Cardiovascular solid mechanics. Cells, tissues, and organs. Springer, New York

Kawasaki T, Sasayama S, Yagi S-I, Asakawa T, Hirai T (1987) Non-invasive assessment of the age related changes in stiffness of major branches of the human arteries. Cardiovasc Res 21:678–687

Ljung L (1999) System identification — theory for the user. 2nd. PTR Prentice Hall, Upper Saddle River

Länne T, Sonesson B, Bergqvist D, Bengtsson H, Gustafsson D (1992) Diameter and compliance in the male human abdominal aorta: influence of age and aortic aneurysm. Eur J Vasc Surg 6:178–184

Nichols WW, O'Rourke MF (2005) McDonald's blood flow in arteries. Theoretical, experimental and clinical principles. Hodder Arnold, London

Peterson LH, Jensen RE, Pernell J (1960) Mechanical properties of arteries in vivo. Circ Res 8:622–633

Rhodin JG (1980) Architecture of the vessel wall. In: Bohr DF, Somlyo AD, Sparks HV (eds) Handbook of physiology, the cardiovascular system, vol. 2, pp 1–31

Ryden-Ahlgren Å, Åstrand H, Sandgren T, Vernersson E, Sonesson B, Länne T (2001) Dynamic behaviour of the common femoral artery: age and gender of minor importance. Ultrasound Med Biol 27:181–188

Schulze-Bauer CAJ, Holzapfel GA (2003) Determination of constitutive equations for human arteries from clinical data. J Biomech 36:165–169

Schulze-Bauer CAJ, Regitnig P, Holzapfel GA (2002) Mechanics of the human femoral adventitia including high-pressure response. Am J Physiol 282:H2427–H2440

Schulze-Bauer CAJ, Mörth C, Holzapfel GA (2003) Passive Biaxial Mechanical Response of Aged Human Iliac Arteries. J Biomech Engrg 125:395–406. doi:10.1115/1.1574331

Singh SI, Devi LS (1990) A study on large radial motion of arteries in vivo. J Biomech 23:1087–1091

Sonesson B, Hansen F, Stale H, Länne T (1993) Compliance and diameter in the human abdominal aorta — the influence of age and sex. Eur J Vasc Surg 7:609–697

Sonesson B, Länne T, Vernersson E, Hansen F (1994) Sex difference in the mechanical properties of the abdominal aorta in human beings. J Vasc Surg 20:959–969

Stålhand J, Klarbring A (2005) Aorta in vivo parameter identification using an axial force constraint. Biomechan Model Mechanobiol 3:191–199

Stålhand J, Klarbring A (2006) Parameter identification in arteries using constraints. In: Holzapfel GA, Ogden RW (eds) Mechanics of biological tissues. Springer, Wien, pp 295–305

Stålhand J, Klarbring A, Karlsson M (2004) Towards in vivo aorta material identification and stress estimation. Biomechan Model Mechanobiol 2:169–186